

# **Validation of numerical analyses on scabbing of reinforced concrete panels subjected to projectile impact**

**Yukihiko Okuda<sup>1</sup>, Zuoyi Kang<sup>2</sup>, Akemi Nishida<sup>3</sup>, Haruji Tsubota<sup>4</sup> and Yinsheng Li<sup>5</sup>**

<sup>1</sup> Assistant Principal Researcher, Japan Atomic Energy Agency, Ibaraki, JAPAN  
(okuda.yukihiko@jaea.go.jp)

<sup>2</sup> Research Engineer, Japan Atomic Energy Agency, Ibaraki, JAPAN

<sup>3</sup> Deputy Division Head, Japan Atomic Energy Agency, Ibaraki, JAPAN

<sup>4</sup> Researcher, Japan Atomic Energy Agency, Ibaraki, JAPAN

<sup>5</sup> Division Head, Japan Atomic Energy Agency, Ibaraki, JAPAN

## **ABSTRACT**

The outer walls of nuclear facility buildings consist of reinforced concrete (RC) panels. When a projectile collides with a nuclear facility building, local damage such as penetration, scabbing, and perforation may occur in the RC panels. Numerical simulation using finite element analysis (FEA) is commonly used to evaluate these damage conditions. However, the impact analysis by FEA modeled with continuum elements makes it difficult to address phenomena such as the scattering of concrete fragments because the element deletion method for large deformations is used to prevent the interruption of numerical calculations.

Recently, a numerical method known as Smoothed Particle Hydrodynamics (SPH), one of the particle methods, has been used to address discontinuous phenomena. In this paper, we focus on the scabbing damage of RC panels and report on the findings obtained through the validation of the numerical analysis using the SPH method.

## **INTRODUCTION**

After the 2011 Fukushima Daiichi Nuclear Power Plant (NPP) accident, new regulatory requirements stipulated by the Nuclear Regulation Authority of Japan were introduced in 2013 for the safety assessment of nuclear facilities subjected to projectile impacts induced by tornadoes or aircraft. To evaluate the influence on the buildings and internal equipment of NPPs due to projectile impact, it is important to develop a local damage evaluation method and confirm its validity using test data.

In recent years, we have experimentally investigated the effects of impact angle and projectile stiffness on local damage to RC panels by conducting impact tests with rigid and soft projectiles in normal and oblique impact directions (Okuda et al., 2022) and reported that oblique impacts caused significantly less damage to RC plates than normal impacts. Referring to a test in which Kojima et al. (1991) investigated the local damage behavior of RC plates by a collision test in which the plates were subjected to normal collisions with projectiles having a hemispherical tip shape, the authors proposed local damage evaluation equations for collisions with rigid and soft projectiles using a hemispherical nose shape. Furthermore, Nishida et al. (2019) used finite element (FE) modeling to simulate the penetration damage of RC plates subjected to oblique impact and evaluated the effect of impact angle. Kang et al. (2019) performed numerical analyses related to oblique impacts by rigid projectiles with flat and hemispherical nose shape geometries to investigate the effect of projectile nose shape on the local damage of RC panels.

This research focused on the scabbing damage of RC panels and compared the experimental and numerical results of normal and oblique impact tests with a soft projectile with a hemispherical nose shape. The scattering of concrete fragments in the scabbing damage is one of the discontinuity phenomena, using a numerical analysis method called SPH (Smoothed Particle Hydrodynamics), which is one of the particle methods. So, the numerical approach in simulating scabbing damage in the RC panel is validated. This paper reports on the findings obtained through the validation of the numerical analysis method for scabbing damage using the SPH method.

## TEST METHOD

### *Impact tests in this study*

The impact angle is the angle between the impact direction of the projectile and the normal direction of the RC panel as shown in Figure 1, and the impact angles of  $0^\circ$  (normal impact) and  $45^\circ$  (oblique impact) were adopted. Figure 2 shows the experimental setup for the normal and oblique impact. The impact tests were conducted using a high-pressure pneumatic projectile launcher with an inner diameter of 200 mm. In the impact test, a projectile ejected from the cannon tube collides with the RC panel installed in a shelter. The RC panel was supported with the support structure through the load cell and flat roller bearings that were designed to slide with extremely low friction parallel to the RC panel. It was constructed to prevent any resistance to movement in the in-plane directions of the RC panel. Table 1 lists the test conditions. Two impact tests were conducted by varying the impact angle.

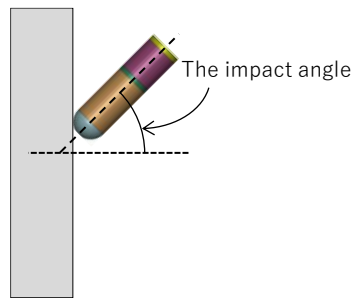


Figure 1. Definition of an impact angle.

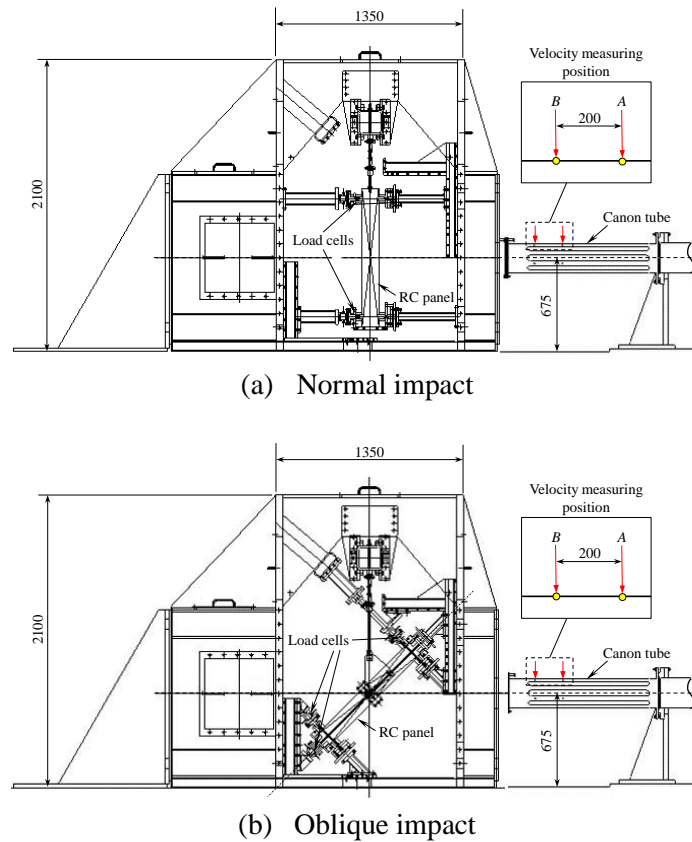


Figure 2. Experimental setup (unit: mm).

Table 1: Test conditions.

Case	Projectile type	Impact angle (°)	Impact velocity (m/s)	Estimated damage mode
1	Soft	0	204	Scabbing
2	Soft	45	206	Scabbing

**RC panels**

The RC panel dimensions were 1000 mm (height) × 1000 mm (width) × 120 mm (thickness) (Figure 3). Figure 4 shows the reinforcement-rebar arrangements of the RC panel. The average concrete compressive strength was approximately 45 N/mm<sup>2</sup>, and the maximum aggregate size was 10 mm.

**Projectile**

The soft projectile used in the tests refers to the reference projectile configurations (Kojima et al., 1991). Figure 5 shows the schematic illustration and views of the projectile used in the tests. The soft projectile was a thin-walled cylinder with 2.2 kg mass, 60 mm diameter, and 235 mm length. The impact velocity was varied to achieve a specific damage mode. The design impact velocity was set at 200 m/s, concerning Kojima et al. (1991).

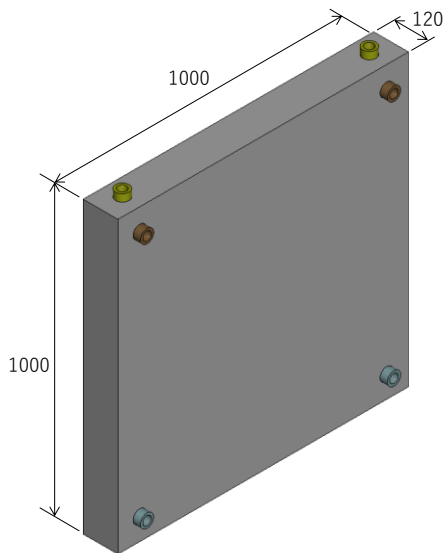


Figure 3. Schematic of the target RC panels (unit: mm).

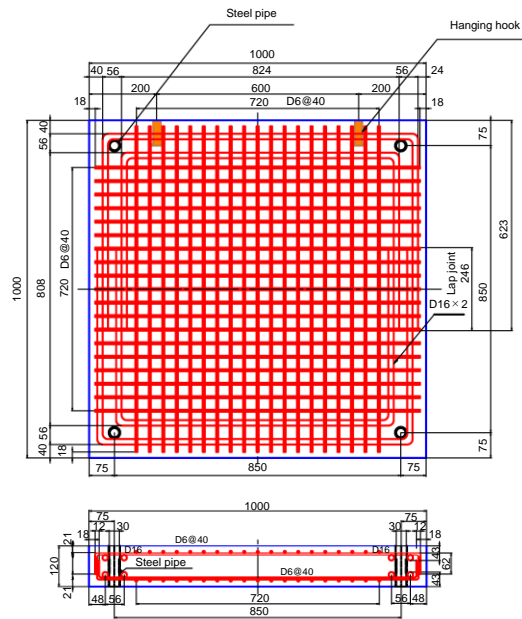


Figure 4. Rebar arrangements of the target RC panels (unit: mm).

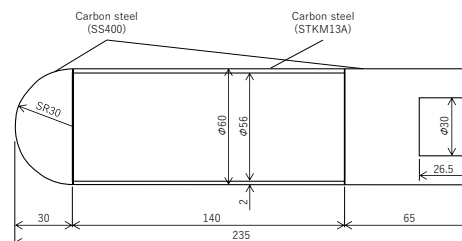
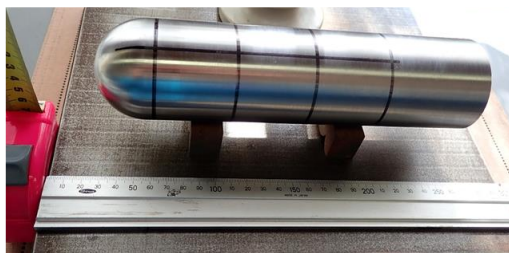


Figure 5. Soft projectile schematics and views (unit: mm).

### Material properties

Tables 2 and 3 list the material properties of the RC panel and the projectiles, respectively. The concrete compressive strength listed in Table 2 was determined based on the average of three concrete compression tests. The material properties of the rebars and projectiles were determined from mill test reports.

Table 2: Material properties of the RC panel.

		Compressive strength (N/mm <sup>2</sup> )	Yield strength (N/mm <sup>2</sup> )	Tensile strength (N/mm <sup>2</sup> )
Concrete		45.0	-	-
Rebar	D6	-	338	507
	D16	-	358	507

Table 3: Material properties of the soft projectiles.

	Yield strength (N/mm <sup>2</sup> )	Tensile strength (N/mm <sup>2</sup> )	Elongation (%)
STKM13A	310	449	54
SS400	320	456	33

### Measuring method

The impact velocity was calculated from the transit time, measured from the different cutting times of two wires for a predetermined 200 mm section of the launcher device shown in Figure 2.

The reaction force acting on the RC panel upon impact was measured using stem-type load cells. The load cells were attached to each RC panel in different arrangements for the normal and oblique impact tests (Fig. 6). In the normal impact test, the reaction force was measured in the out-of-plane direction at four points (i.e., L1–L4) corresponding to each corner of the RC panel. In the oblique impact test, the component forces in the out-of-plane and in-plane directions of the RC panel must be divided, and each reaction force must be measured separately. The reaction force of the oblique impact test was measured at six measurement points (L1–L6), including the out-of-plane (L1–L4) and in-plane (L5 and L6) directions. The load cell capacity was approximately 1,000 kN per piece, which was sufficient for the reaction force measured in the impact tests. In addition, an initial compressive load of 40 kN was applied at each support point to accurately record the tensile reaction force with compression load cells. The impact behavior at the impact face and the damage behavior of the RC panel were recorded using two high-speed cameras. One was installed on the front side (impact side) and the other on the rear side of each RC panel.

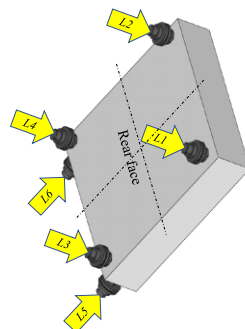


Figure 6. Measurement locations of the reaction force using load cells.  
 (Normal impact: L1-L4, Oblique impact: L1-L6)

## ANALYTICAL MODEL

### RC panel

We investigated the applicability of the so-called Winfrith model, Karagozian & Case Concrete (KCC) model, and CSCM model in LS-DYNA to evaluate the local damage of RC panels subjected to projectile impact. Winfrith model is a basic plasticity model that includes the third stress invariant for consistent treatment of triaxial compression and extension. KCC model and CSCM model are parameter automatically generated material models for simulation by giving the unconfined compressive strength of the concrete. Although there was no obvious difference in the evaluation of damage zones among the three models, the CSCM model was finally adopted because of its ability to provide stable analysis results. The FE model of RC panels is composed of first-order hexahedral reduced integration solid elements for concrete. The material properties of the concrete defined in the RC panel are shown in Table 4. The compressive strength and Young's modulus of concrete were tested using three cylindrical specimens, and the average value was adopted.

Table 4: Material properties of concrete for FEA.

	unit	Value
Compressive strength	MPa	45
Tensile strength	MPa	3.757
Young's modulus	MPa	26300
Aggregate size	mm	10

In addition, an uneven mesh size was adopted to capture the dynamic behavior of an RC panel around the impact zone and reduce the computation time. As shown in Figure 7, we used the fine mesh of 5 mm around the impact zone, and the coarse mesh of approximately 10~20 mm was set in an area away from the impact center. For the area around the impact zone, the rear part of the RC panel cross-section (16 mm thickness) was modeled with SPH elements to simulate the scattering of concrete fragments, while the front face was a first-order hexahedral reduced integral solid element.

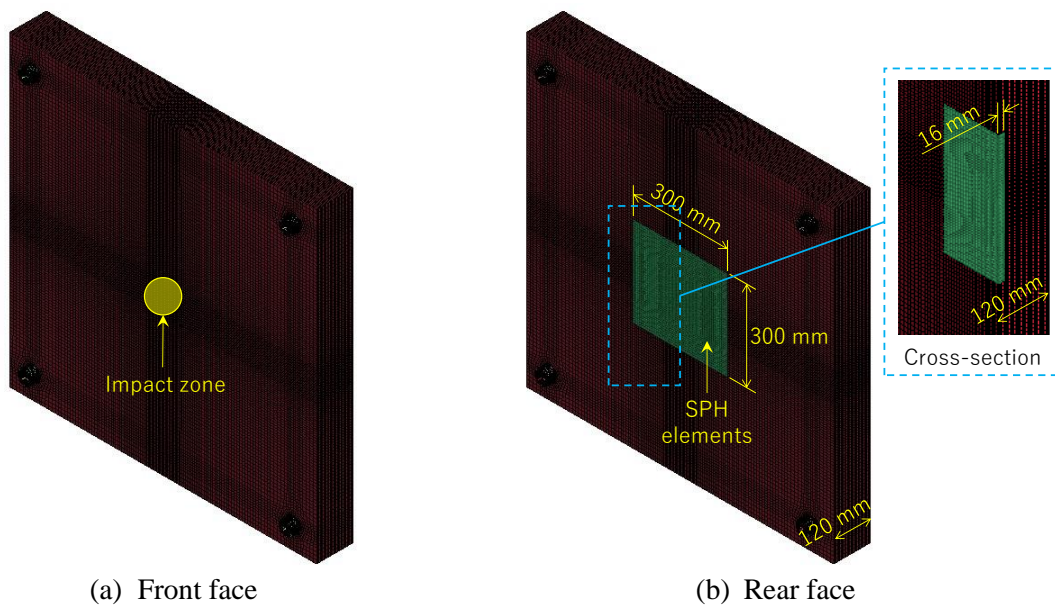


Figure 7. Mesh of RC Panel.

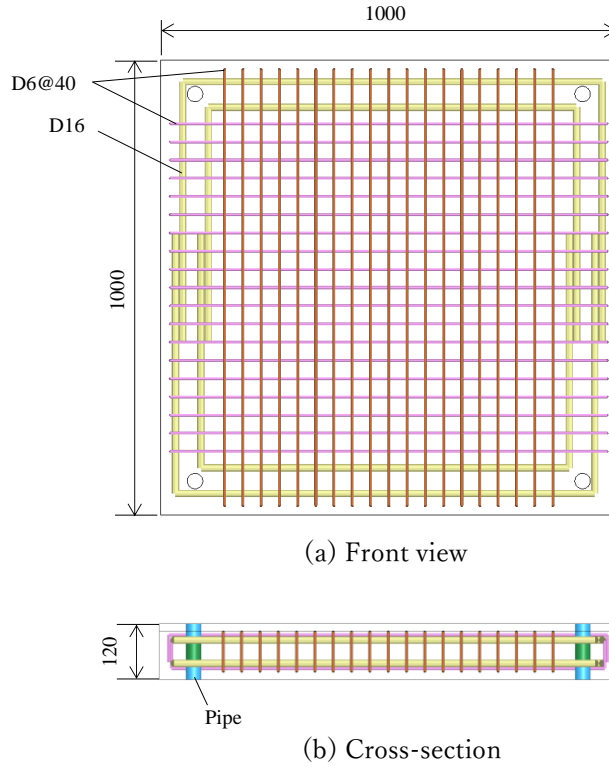


Figure 8. Steel rebar (unit: mm).

Gaussian-point integration beam element for steel rebar was used and they were arranged as shown in Figure 8. In order to represent the interaction behavior between concrete and steel rebar, the beam elements were embedded inside the concrete solid elements. The material properties of steel rebar D6 and D16 used in the RC panel are shown in Table 3. The material properties of the steel rebar were determined from the mill test reports. The threshold for numerical erosion was set at 20% based on the material test results. The effect of strain rate was considered for the steel rebar by applying the WES formula defined in WES-2808 (2013).

$$\sigma_y = \sigma_{y0}(T_0) \cdot \exp \left[ 8 \times 10^{-4} \cdot T_0 \cdot \left( \frac{\sigma_{y0}(T_0)}{E} \right)^{-1.5} \cdot \left\{ \frac{1}{T \cdot \ln(10^8/\dot{\epsilon})} - \frac{1}{T_0 \cdot \ln(10^8/\dot{\epsilon}_0)} \right\} \right] \quad (1)$$

### Projectile

The soft projectile was modeled using solid elements for the front and rear parts. The cylinder part adopted the fully integrated first-order shell element. We considered the shared node to connect the solid and shell elements. The material properties of the projectile are shown in Table 4. The soft projectile was made of steel SS400 in Japanese Industrial Standard (JIS) and STKM 13A in JIS, as shown in Figure 9. The WES formula defined in WES-2808 was applied to determine the strain rate effects for the projectile materials (WES 2808, 2013). The soft projectile was accelerated to impact the RC panel following the center of the RC panel at a design impact velocity of 200 m/s.

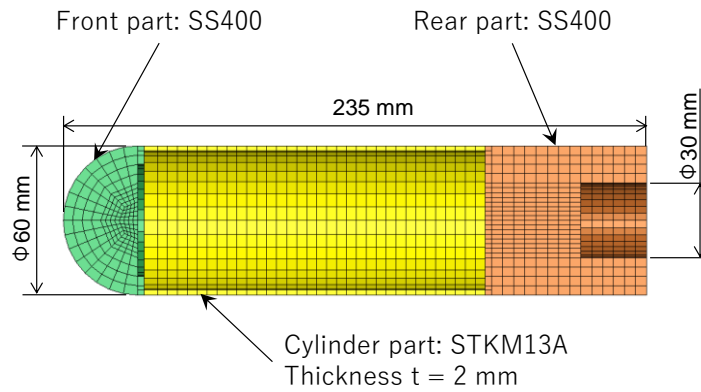


Figure 9. Soft projectile

## ANALYTICAL CONDITIONS

### *Detailed modeling of constraint conditions*

As shown in Figure 10, the ends of the load cells on the rear and lower sides of the RC panel were restrained to provide boundary conditions and spring elements were set. The spring constants of the supports are shown in Figure 10.

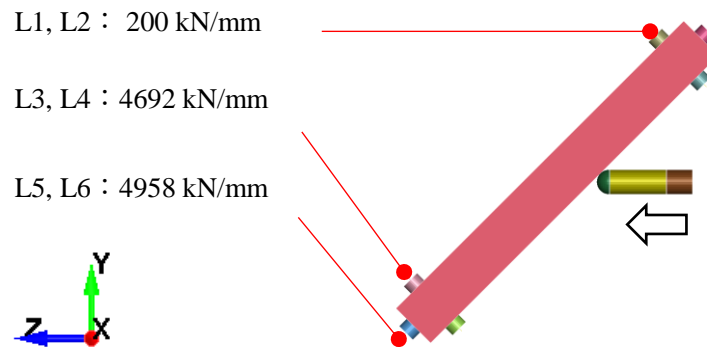


Figure 10. Spring constants of the supports.

### *Contact conditions*

In this study, four types of contact conditions were considered for the projectile and concrete, projectile and rebar, and self-contact of the projectile. In addition, the friction coefficient for each contact condition referred to generic values that are widely used in contact calculations (Maruzen, 1977), as summarized in Table 4.

Table 4: Definition of contact conditions.

Object	Contact condition	Friction coefficient
Projectile–concrete	Surface to surface	0.3
Projectile–rebar	Node to surface	0.2
Self-contact of projectile	Single surface	0.2
Support- concrete	Node to surface	0.3

## RESULTS AND DISCUSSIONS

### *Damage mode of RC panel*

Figure 11 shows the comparisons of scabbing damage to the rear face of the RC panels between test and simulation analysis results using the SPH method in normal and oblique impact. Based on the results of this comparison, it was confirmed that the SPH method is effective in the scattering of concrete fragments of scabbing damage.

Figure 12 shows the comparisons of scabbing damage on the front face of the RC panels between the test and simulation analysis results. Comparing the surface test results with the simulation analysis results, differences were observed in the damage area. This may be due to the material property of the concrete model considered in the simulation analysis. In particular, the concrete material model and the numerical erosion threshold should be examined in detail.

### *Reaction force*

Figures 13 and 14 show the time histories of the reaction forces compared between the test and simulation analysis results. The contact time between the concrete and the projectile was set to  $t=0\text{ms}$ . The compression of the reaction force is positive. The reaction forces of the normal impact test represent the sum of L1 to L4 in the normal direction. The reaction forces of the oblique impact test represent the sum of L1 to L4 and from L5 to L6 in the normal and in-plane directions, respectively. The filtered time history is shown in the test results to remove the time history disturbance, which was considered to be electrical noise. The maximum reaction forces were in agreement between the test and the simulation analysis. Regarding the vibration characteristics of the reaction forces, the analytical results tend to have a higher frequency than the test results, which is an issue to be addressed in the future.

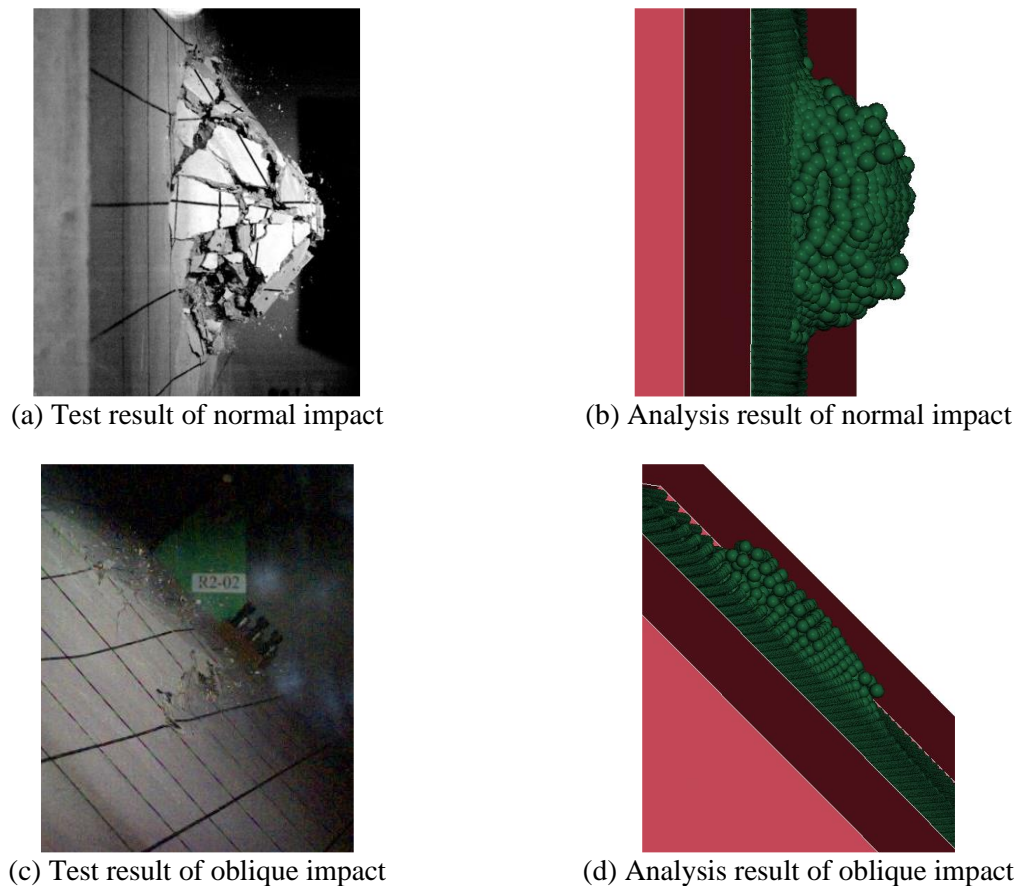
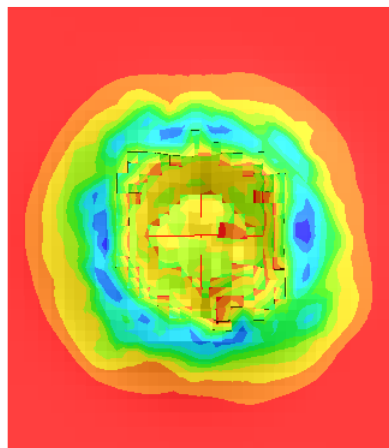


Figure 11. Comparisons of scabbing damage to the rear face of the RC panels using the SPH method.



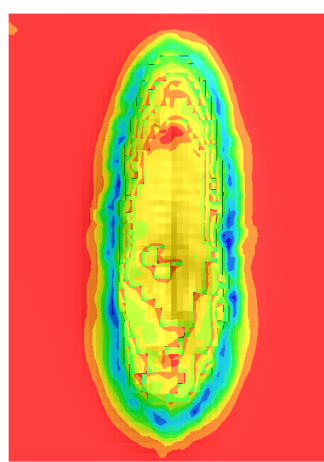
(a) Test result of normal impact



(b) Analysis result of normal impact



(c) Test result of oblique impact



(d) Analysis result of oblique impact

Figure 12. Comparisons of scabbing damage to the front face of the RC panels.

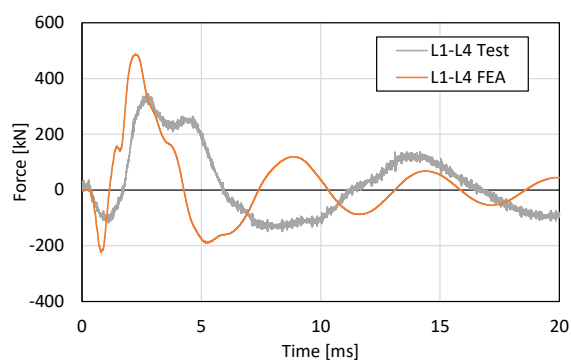


Figure 13. Time histories of the reaction force (normal impact).

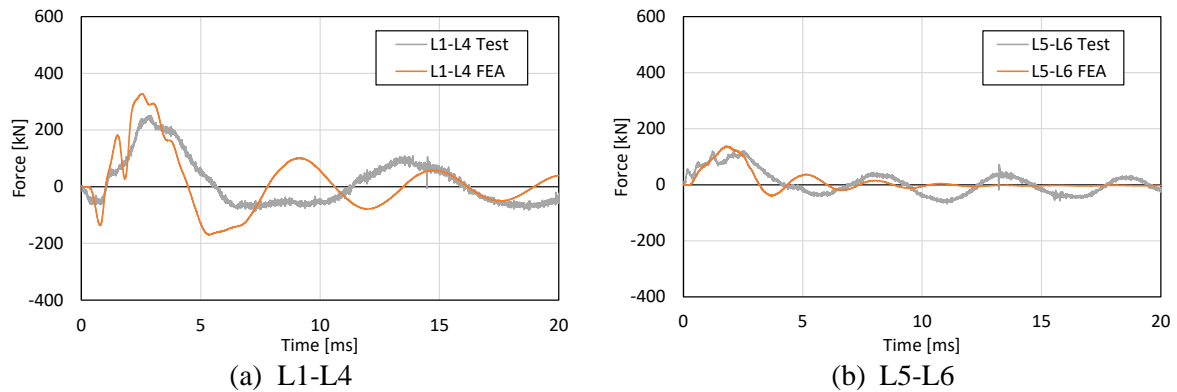


Figure 14. Time histories of the reaction force (oblique impact).

## SUMMARY

This study conducted the validation of the numerical analysis method for scabbing damage using the SPH method, and the following was observed from the numerical analysis results compared with the test results.

- Based on the results of this comparison, it was confirmed that the SPH method is effective in the scattering of concrete fragments of scabbing damage.
- Comparing the surface test results with the simulation analysis results, differences were observed in the damage area. This may be due to the material property of the concrete model considered in the simulation analysis. In particular, the concrete material model and the numerical erosion threshold should be examined in detail.
- The maximum reaction forces were in agreement between the test and the simulation analysis. Regarding the vibration characteristics of the reaction forces, the analytical results tend to have a higher frequency than the test results, which is an issue to be addressed in the future.

We intend to perform a detailed analysis concerning the concrete material model and the numerical erosion threshold based on some material test data.

## REFERENCES

- Kojima, I. (1991). "An Experimental Study on Local Behavior of Reinforced Concrete Slabs to Missile Impact," Nucl. Eng. Des., Vol. 130, pp.121-132.
- Kang, Z., Okuda, Y., Nishida, A., Tsubota, H. and Li, Y. (2022). "Local damage to reinforced concrete panels subjected to oblique impact by projectiles; Numerical analysis on test results", ICONE29-88884, 29th International Conference on Nuclear Engineering; Nuclear Energy the Future Zero Carbon Power (ICONE 29), 8/8-12, Shenzhen, China.
- Kang, Z., Okuda, Y., Nishida, A., Tsubota, H. and Li, Y. (2022). "Investigation on Local Damage of Reinforced Concrete Panel Impacted by Hemispherical Soft Projectile", ICONE30-1677, 30th International Conference on Nuclear Engineering (ICONE 30), 5/25-30, Kyoto, Japan.
- Maruzen, (1977), Architecture Handbook II – Structure –, 2nd edition, (in Japanese).
- Okuda, Y., Nishida, A., Kang, Z.Y., Tsubota, H. and Li, Y. (2022). "Experimental study on local damage to reinforced concrete panels subjected to oblique impact by projectiles," ASME J. of Nuclear Rad. Sci. 2023, Vol. 9(2): 021801, pp.1-12.
- Okuda, Y., Kang, Z., Nishida, A., Tsubota, H. and Li, Y. (2023). "Experimental study on scabbing limit of local damage to reinforced concrete panels subjected to oblique impact by projectile with semispherical nose," Mechanical Engineering Journal, Vol.10, No.3.
- WES 2808. (2013). Method of assessing brittle fracture in steel weldments subjected to large cyclic and dynamic strain, The Japan Welding Engineering Society, Japan.